

CONVECTIVE BOILING HEAT TRANSFER IN A CONCENTRIC ANNULAR GAP†

A. SHARON,¹ L. CHEN² and S. G. BANKOFF³

Chemical Engineering Department, Northwestern University, Evanston, IL 60201, U.S.A.

(Received 10 March 1983; in revised form 10 March 1983)

Abstract—Heat transfer and pressure drop characteristics were measured in both subcooled and saturated concentric narrow gap forced convection boiling. Four boiling regimes were observed: isolated bubbles, coalesced bubbles, coalesced bubbles with small dry patches, and liquid deficient flow. Data were obtained to qualitatively identify the effects of gap size, pressure, flow rate, inlet quality and wall superheat on the boiling regimes and the transitions between the various regimes. Some significant differences from unconfined forced convection boiling were found.

1. INTRODUCTION

Problems of tube denting and thermal stress corrosion in PWR steam generators are postulated to result, in part, from intermittent localized dryout in the narrow crevices between the tubes and the tube support plate (TSP) (Baum & Curlee 1980). In the older steam generators this crevice is typically annular, although more recent designs employ other shapes to minimize the dryout problem. We concern ourselves here with circular holes in the TSP.

Four different tube-TSP geometries can result, as shown in figure 1:

(a) *Line contact* between the heated tube and the support plate. Heat transfer in this geometry has been studied and analyzed by Bankoff *et al.* (1982). It was found that a stable dry patch exists around the contact line at a tube wall superheat of 2–3°C. The extent of the dry patch was typically about 15° on either side of the contact line. Changes in flow rate and inlet enthalpy were found to have little effect on the patch extent or contact line temperature, but an increase in gap size decreased both.

(b) *Point contact*. To our knowledge, no studies have been made to date in this geometry, except possibly because of imperfect alignment.

(c) *Eccentric gap*. Bankoff *et al.* (1982) observed that separating the tube and TSP by about 0.025 mm allows the dry patch to rewet.

(d) *Concentric gap*. This is the subject of the present study. With line contact large circumferential temperature gradients exist, and the vapor released from the dry patch region has a strong tangential velocity component. In the concentric gap, on the other hand, no circumferential variations in velocity and temperature are expected.

Ishibashi & Nishikawa (1969) studied saturated pool boiling in a vertical concentric annulus, utilizing an electrically-heated inner tube, over the following parameter ranges:

Gap size: 1–20 mm

Pressure: 0.1–1.1 MPa

Liquids: distilled water, various surfactant solutions, and ethyl alcohol

Heat Flux: 0.8–70 kw/m².

Two fundamentally different boiling regimes were identified. The first was the *isolated bubble regime*, which is little different in appearance from normal pool boiling. The heat transfer coefficient was found to increase with pressure and decreasing heat flux. The other was the

†Work supported by a contract with the Electric Power Research Institute, Palo Alto, California.

¹Visiting Scholar, 1981. Present address: Fauske & Associates, Inc. 16W070 West 83rd Street, Burr Ridge, IL 60521, U.S.A.

²Visiting Scholar, 1980–1982. Present address: Power Engineering Department, Xi'an Jiaotong University, Xi'an, Shaanxi Province, The People's Republic of China.

³To whom communications should be addressed.

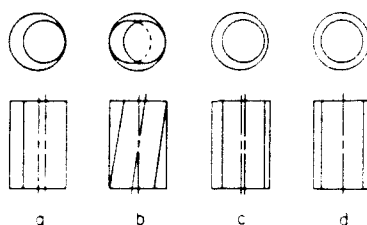


Figure 1. Schematic description of possible tube-tube support plate geometries. (a) line contact; (b) point contact; (c) eccentric gap; and (d) concentric gap.

coalesced bubble regime, in which large bubbles filled the crevice, leaving a liquid film on the heater surface and departing at a slow regular frequency of about 0.5 sec. The departure frequency increased with heat flux and decreased with pressure and gap size. The heat transfer coefficient in this boiling regime decreased with pressure. This was attributed to the decrease in departure frequency with pressure, but might simply be due to the slower bubble growth. Another interesting observation was that in the coalesced bubble regime neither the emission frequency nor the heat transfer coefficient were affected by surface tension. By decreasing the gap size or increasing the heat flux, it was possible to obtain a liquid-deficient condition, with large temperature oscillations. In this regime the heat transfer coefficient was found to decrease or to be almost unaffected as the heat flux increased. The transition between the isolated bubble regime and the coalesced bubble regime took place at a gap size of 3 mm at atmospheric pressure, which decreased to about 0.7 mm at a pressure of 0.5 MPa.

The present investigation deals with the heat transfer characteristics and pressure drop in forced-convection boiling in a narrow concentric annular gap, both under subcooled and saturated inlet conditions. In this paper only visual observation and qualitative trends of the data are reported. More detailed quantitative results will be presented at a later stage.

2. EXPERIMENTAL

The test system consists of a single 19.05 mm (0.75 in) tube passing through a drilled hole in a tube support plate made of quartz. As a result it was possible to observe the boiling and flow phenomena. Two support plates were used with hole diameters of 19.685 and 19.431 mm, such that the gap sizes were 0.317 and 0.191 mm, respectively. The plate thickness was 19.05 mm.

The tube was heated by a downward flowing water stream in the primary loop. This water was pressurized with nitrogen to 1.8 MPa. The primary water temperature could vary up to 205°C and was controlled by a 10.5 kw heater. A schematic diagram of the experimental apparatus is shown in figure 2. The secondary flow loop was pressurized with its own vapor up to a pressure of 0.8 MPa. The secondary inlet quality was controlled by a 12 kw preheater and its flow rate was manually controlled by a valve between the flow orifice meter and the preheater.

The two loops were entirely separate, interacting only to exchange heat in the test section. Each was heated, cooled, pumped and metered independently. Each was filled with water treated in a fabric filter, charcoal filter, and two ion-exchange columns. The entire flow loop was constructed of type 304 and 316 stainless steel. In the wall of the tube were embedded four 0.51 mm OD steel-sheathed thermocouples. The junctions were located within the region of the annular crevice. Thus, both visual observations and wall temperature measurements were available.

To assure concentricity of the gap between the tube and the TSP, two spacer wires, 90° apart, were inserted into the gap. The plate was pushed to the tube and held in place by four micrometers, 90° apart. The gap uniformity was rechecked with spacer wires. Since tube out-of-roundness was measured to be 0003 mm a uniform gap was established.

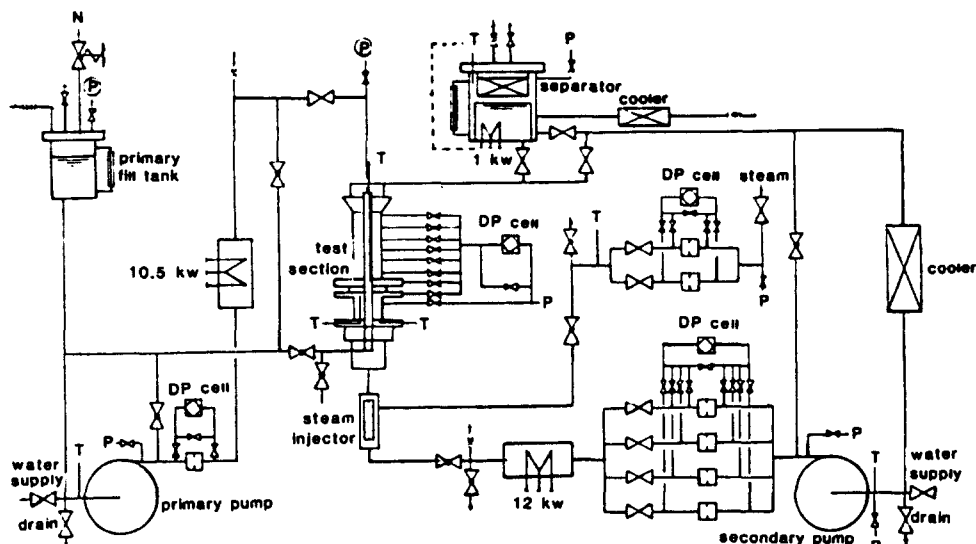


Figure 2. Schematic diagram of experimental apparatus, taken from Bankoff *et al.* (1982).

For a particular support plate, an experimental run involved setting the secondary flow rate, pressure and inlet enthalpy, and maintaining these while varying the primary water temperature. The experiment began with the primary temperature close to that of the secondary. The primary temperature was increased in several steps up to a maximum of 205°C (pump temperature limit). When steady-state had been reached, the temperature, flow rates, and pressure drop were recorded.

The following experimental parameters were covered:

- Pressure: 0.13–0.7 MPa
- Mass velocity: 570, 330 kg/sm²
- Inlet quality to test section: –0.05 (15°C subcooling) to +0.15.

The experimental matrix is described in table 1.

3. EXPERIMENTAL RESULTS

Visual observation and the trends of the present data demonstrate some significant differences from other boiling modes. Namely: (a) unconfined forced convective boiling; (b) narrow gap pool boiling (Ishibashi & Nishikawa 1969); and (c) narrow gap forced-convection boiling with a line contact (Bankoff *et al.* 1982).

The results described below are primarily aimed at pointing out the differences in heat transfer and pressure drop characteristics and identifying the boiling regimes occurring in this forced-convection, concentric annular gap boiling.

The heat transfer data were analyzed by constructing boiling curves for each run. These curves are plots of the heat flux vs the temperature difference between the outer tube surface temperature and the saturation temperature. In cases where the pressure drop was large, the saturation temperature was calculated based on the exit pressure of the gap. The pressure drop data were used to calculate the two-phase pressure drop multiplier, defined as the ratio between the actual two-phase pressure drop to the pressure drop for water flow at the same mass velocity and flow area.

As shown in table 1, experimental data were taken for both subcooled and saturated inlet conditions. Due to the differences in boiling characteristics between the two cases all the following discussions will consider each of them separately.

Table 1. Experimental conditions

Run	Gap mm	Pressure Bar	Mass Velocity kg/s m ²	Inlet Quality (Subcooling)
20	0.317	3.0	570	0.0
21		3.0	570	+0.142
22		3.0	570	-0.035 (12°C)
23		3.0	330	-0.057 (14°C)
24		3.0	330	+0.075
25		7.1	330	-0.045 (13°C)
26		7.1	570	-0.01 (8°C)
27		7.1	330	-0.005 (2°C)
28		1.3	330	+0.14
29		1.3	330	-0.037 (8°C)
30	0.191	1.3	550	-0.07 (14°C)
31		1.3	330	+0.14
32		3.0	330	+0.14
33		3.0	330	0.0

3.1 Visual observations

Unlike the case of narrow gap boiling with line contact no stable dry patches were observed. The flow was parallel to the tube axis; no circumferential variations in temperature or boiling appearance were found.

In spite of the small gap size, which should have resulted in only coalesced-bubble boiling according to Ishibashi & Nishikawa (1969) it was possible to identify isolated bubbles even in the 0.191 mm gap and at a pressure of 0.3 MPa.

Four different boiling regimes were identified:

(a) *Isolated bubble regime*. In this case the wall temperature is steady and close to the secondary water saturation temperature.

(b) *Coalesced bubble regime with steady wall temperature*. Large vapor bubbles are observed in the gap and the wall temperature is higher.

(c) *Coalesced bubble regime with oscillating wall temperature*. Small dry patches are momentarily formed on the tube wall and swept away immediately.

(d) *Liquid deficient regime*. Larger dry patches with longer lifetimes (0.5–5 sec) are formed, with liquid flowing as rivulets or entrained droplets.

The schematic relations between the visual boiling regime observations and the temperature readings are described in figure 3.

3.1.1 *Subcooled inlet conditions*. In the case of subcooled inlet conditions, small bubbles formed on the tube surface for all cases where the wall temperature slightly exceeded the saturation temperature. However, as the wall temperature increased a coalesced bubble regime was observed, with large vapor bubbles forming which were swept vertically away. With a 0.317 mm gap and subcooled inlet conditions this boiling regime prevailed even for high primary water temperatures (heat fluxes of about 0.3–0.5 Mw/m²). In this case large bubbles were formed at a low frequency ($\sim 0.2\text{--}1\text{ s}^{-1}$), leaving a thin liquid film on the tube surface. No dry patches formed and consequently the wall temperature was steady in most cases of subcooled boiling in a 0.317 mm gap. Only in one run (No. 29), at low pressure and flow rate, but high heat

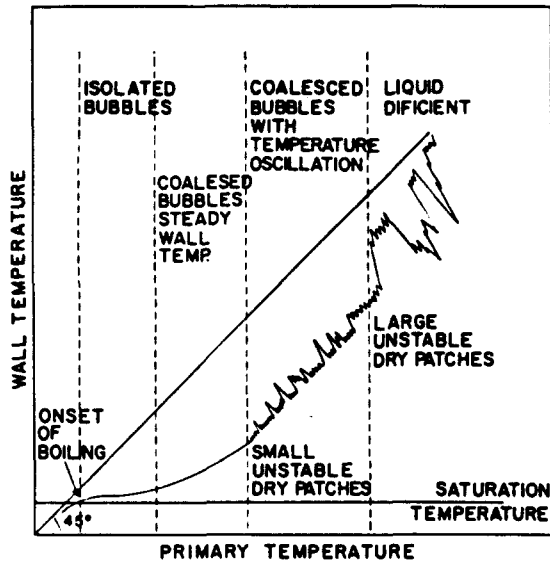


Figure 3. Schematic description of boiling regimes in concentric annular gap.

flux (0.5 Mw/m^2), were some dry regions formed which were unstable. This resulted in some small surface temperature oscillations with a frequency of about 1 sec.

With a 0.191 mm gap several differences were observed:

(a) The transition between the isolated bubble and coalesced bubble boiling regimes occurred at a lower wall superheat.

(b) Unsteady dry patches occurred even at a higher mass velocity (Run 30) and lower primary temperature (150°C , 0.24 Mw/m^2). Large amplitude, high-frequency temperature oscillations were observed.

(c) The liquid deficient boiling regime was observed at a wall temperature slightly above the wall temperature at which unsteady dry patches formed. This boiling regime is characterized by large dry patches that might contain some entrained liquid droplets or rivulets. Those patches remain on the tube surface for a relatively long time (2–5 sec), and then are swept away, leading to tube rewetting. The wall temperature shows large amplitude oscillations, with peak temperature approaching the primary liquid temperature.

3.1.2 Saturated inlet conditions. With 0.317 mm gap and relatively low subcooling (negative quality 0.075, Run 24), vapor enters the gap as isolated bubbles. When the wall superheat is small (up to $\sim 5^\circ\text{C}$) the wall temperature was stable and isolated bubble boiling was observed. Increasing the wall superheat above $\sim 5^\circ\text{C}$ results in a transition to coalesced-bubble boiling. The wall temperature begins to oscillate and small vapor patches are formed. For higher wall superheats ($\sim 15^\circ\text{C}$ and above) the transition to liquid-deficient boiling occurs, with large dry patches formed on the tube with lifetimes of about 0.6–2 sec. However, with larger inlet quality (0.14)—(Run 21), coalesced boiling is observed even at a low wall superheat (2.2°C), with vapor entering the gap as slugs rather than as small bubbles. The wall temperature oscillates with increased amplitude and frequency as the wall superheat increases.

On the other hand, with a 0.191 mm gap, vapor enters the gap in slugs, even when the inlet quality is only slightly above zero. The transition to liquid-deficient boiling occurs at a lower wall superheat, as compared with the larger gap under similar conditions.

3.2 Gap heat transfer

3.2.1 Subcooled inlet conditions. For a small positive wall superheat nucleate boiling will

start on the tube surface. The onset of boiling occurs at wall superheats typically in the range of 0.5–5°C. For the smaller gap, onset of boiling occurs at a very low wall superheat ($\sim 0.2^\circ\text{C}$), while for the larger gap this value is typically around 3°C . Lower pressures and larger flow rates tend to decrease this temperature difference. The onset of boiling is marked by ONB in figures 4–6.

The effects of mass velocity, pressure and gap size on the boiling curves are shown in figures 4–6, respectively. Mass velocity has no effect on the boiling curve at low wall superheat, as shown in figure 4. At a large wall superheat ($\sim 20^\circ\text{C}$), however, the wall temperature started to oscillate at the smaller flow rate, leading to apparently lower heater fluxes.

The effect of pressure on the boiling curve is rather interesting. As shown in figure 5, at the lower wall superheats and higher pressures, it has only a small effect. However, the heat flux is greater at 0.13 MPa, probably due to earlier boiling incipience and transition to coalesced-bubble boiling. This finding of decreasing heat transfer coefficient with pressure in the coalesced-bubble boiling regime is in agreement with the pool boiling data of Ishibashi & Nishikawa (1969).

Smaller gap size improved heat transfer at low wall superheats (figure 5). However, above some ΔT the opposite trend was observed. This phenomenon was attributed to the transition to coalesced bubbles, with increased void fraction in the gap.

3.2.2 Saturated inlet condition. As shown in figure 7 for a pressure of 0.3 MPa, increasing the inlet quality actually improves the heat transfer for low wall superheats ($\Delta T < 12^\circ\text{C}$) with a 0.317 mm gap. There is a nearly linear relation between q and ΔT in this range which flattens out at some critical ΔT . This transition is probably due to the increased void fraction in the gap leading to the formation of short-duration dry patches. It is interesting to note that this

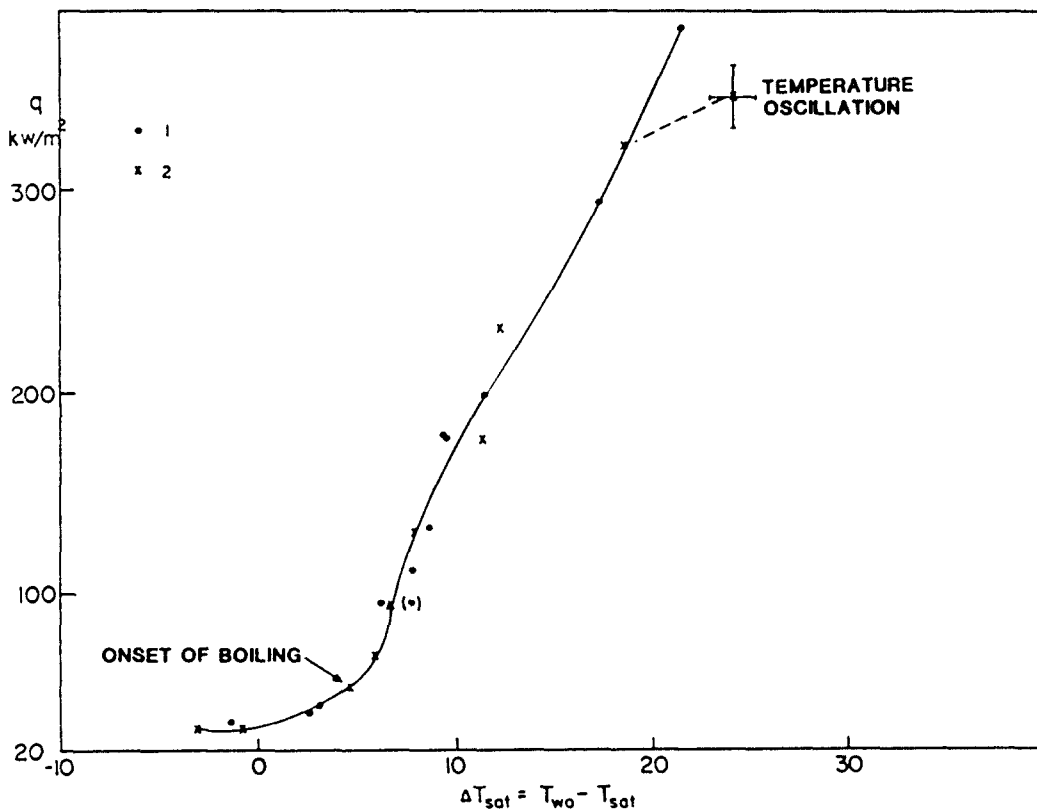


Fig. 4. Subcooled concentric gap boiling curves for different mass velocities.

Symbol	G , $\text{kg/m}^2\text{s}$	T_{sub} , $^\circ\text{C}$	Pressure, 10^5 n/m^2	Gap, mm
1	570	12	3.0	0.317
2	330	14	3.0	0.317

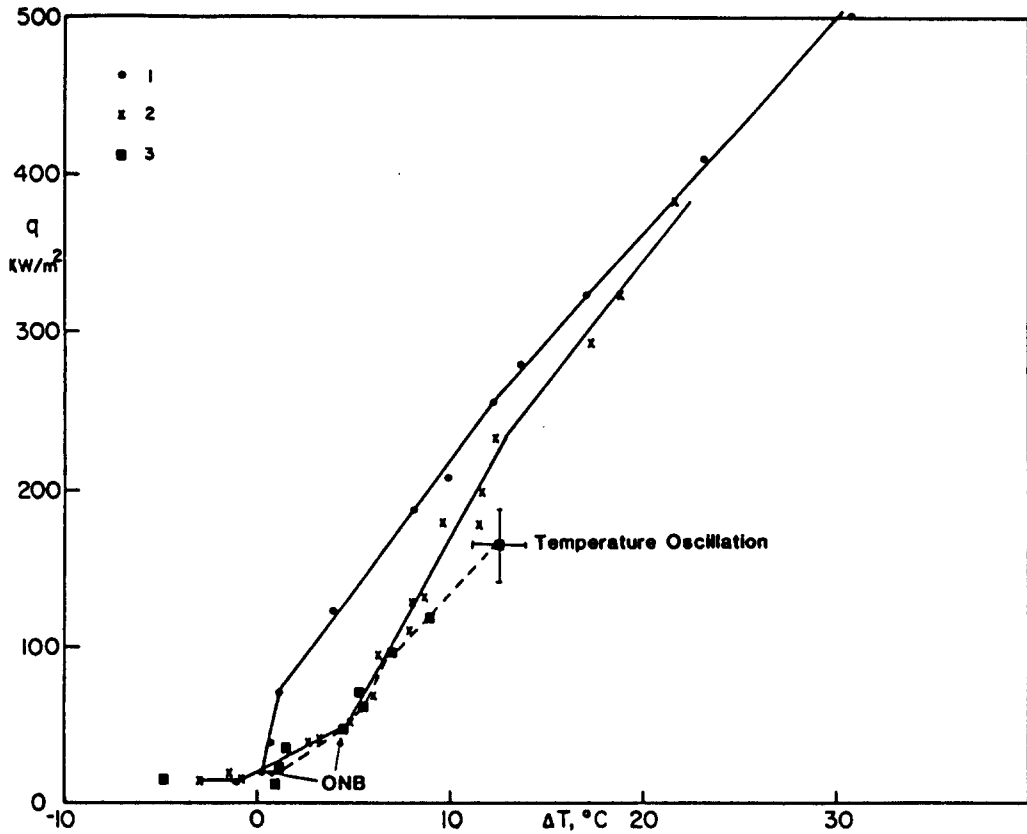


Fig. 5. Effect of pressure on subcooled concentric gap boiling.

Symbol	$G, \text{kg/m}^2\text{s}$	$T_{\text{sub}}, \text{°C}$	Pressure, 10^5 n/m^2	Gap, mm
1	330	8	1.3	0.317
2	570,330	12-14	3.0	0.317
3	570,330	8-13	7.1	0.317

transition is a function of inlet quality; as the quality increases the critical ΔT is decreased. The same effect is found at a pressure of 0.71 MPa with an inlet quality near zero. On the other hand, at the lowest pressure (0.13 MPa) and a lower mass velocity ($330 \text{ kg/m}^2\text{s}$), increasing the inlet quality results in a lower heat flux, as shown in figure 8. This is probably due to the higher void fraction at lower pressure. With a smaller gap this phenomenon is even more pronounced, as one might expect.

The effect of gap size at high inlet qualities is shown in figure 9. A smaller gap results in a smaller heat flux, due to the coalesced bubbles effect, and the liquid deficient regime is obtained at high ΔT . The transition to this regime occurs when the maximum in the boiling curve is attained, leading to an apparent critical heat flux behavior.

In the range of 0.1–0.7 MPa and large inlet quality ($x \sim 0.14$) no particular pressure effects were noticed.

The effect of mass velocity is shown in figure 7. Due to the enhanced coalesced-bubble effect at low mass velocities, the heat transfer coefficient increases more slowly with respect to ΔT , and decreases with decreasing mass velocity at high ΔT .

Another interesting result was obtained when an experimental run was carried out with constant primary water temperature and flow rate. The secondary heater duty was set to a constant value and the secondary flow rate was decreased in small steps. In this case, the combined effect of mass velocity and quality is observed. This procedure can be adapted to

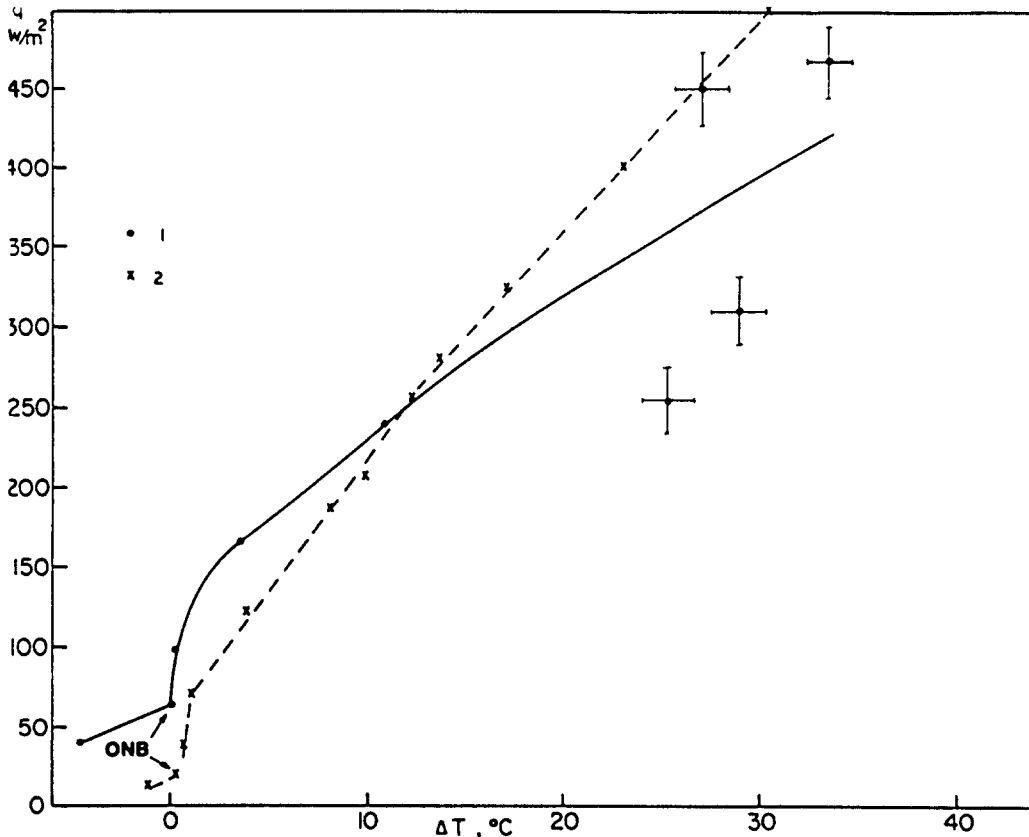


Figure 6. Effect of gap size on subcooled concentric gap boiling.

Symbol	G , $\text{kg/m}^2\text{s}$	ΔT_{sub} , $^{\circ}\text{C}$	Pressure, 10^1 n/m^2	Gap, mm
1	330	~ 8	1.3	0.191
2	570	8	1.3	0.317

determine the transition to unstable dry patch formation. The results are shown in figure 10. For $G > 500 \text{ kg/m}^2\text{s}$ single-phase heat transfer is obtained, but as G decreases, nucleate boiling begins, leading to an increase in heat flux. As the boiling heat transfer becomes dominant, the heat flux becomes independent of G . However, as G is further decreased, unstable dry patches are formed, leading to wall temperature oscillation, and hence to a decrease in heat flux.

When comparing these narrow-gap heat transfer coefficients with those of the Chen correlation (Collier 1981), the narrow-gap coefficients are smaller by a factor of about three, except for the liquid-deficient regime, where the deviations are much larger.

3.3 Pressure drop

3.3.1 Subcooled inlet condition. Data for pressure drop vs heat flux are shown in figure 11. The effects of pressure and mass velocity are clearly demonstrated. Increasing mass velocity and decreasing pressure (decreasing mixture density) both increase ΔP ($\Delta P \propto G^2/\rho$).

For subcooled boiling the pressure drop data are typically plotted as the two-phase multiplier ϕ vs the relative heat flux q''/q''_{sat} . q'' is the actual heat flux while q''_{sat} is the heat flux required just to produce saturated boiling at the exit of the test section (Collier 1981). The two-phase pressure drop multiplier is calculated as the ratio of the actual pressure drop divided by the measured pressure drop for water only flowing at the same mass velocity. q''_{sat} was

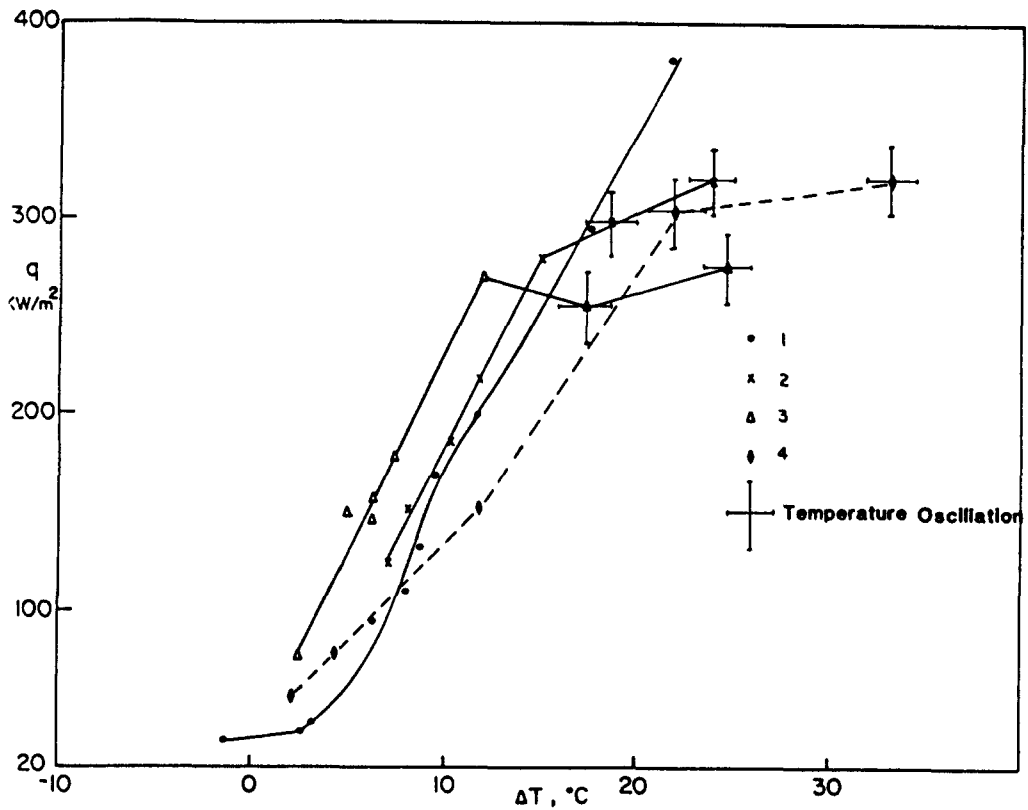


Figure 7. Effect of inlet quality and mass velocity on concentric narrow gap boiling.

Symbol	$G, \text{kg/m}^2\text{s}$	Inlet quality	Pressure 10^4 n/m^2	Gap, mm
1	570	-0.04	3.0	0.191
2	570	0.0	3.0	0.191
3	570	0.142	3.0	0.191
4	330	0.07	3.0	0.191

calculated by

$$q''_{\text{sat}} = \frac{(-x_{\text{in}})\dot{M} h_{L,G}}{A} \tag{1}$$

where \dot{M} is the mass flow rate, $h_{L,G}$ is the latent heat and A the area for heat transfer. A plot of ϕ^2 vs q''/q''_{sat} is shown in figure 12 for various flow rates and pressures. A curve of this nature might well serve to illustrate the trend of the data. The deviations of the experimental data from the curve can be attributed, at least in part, to the uncertainties in q''_{sat} due to the experimental error band ($\sim 10\%$). When comparing figure 12 to a similar plot for tube flow, (Collier 1981, p. 196) it is observed that the pressure drop increases continuously with q'' , rather than decreasing at small q'' and increasing at larger q'' . For subcooled unconfined convective boiling this decrease may be explained by a lubricating effect of the bubbles at small heat fluxes, reducing the effective wall viscosity and consequently the wall shear. In subcooled narrow-gap boiling this effect does not exist.

3.3.2 Saturated inlet conditions. In this case ϕ^2 is a function of quality in unconfined convective boiling (Collier 1981). Since the quality increase in the gap may be large, the average quality, \bar{x} , is used in plotting the data. Plots of ϕ^2 vs \bar{x} at various pressures, gap widths and flow rates are shown in figure 13.

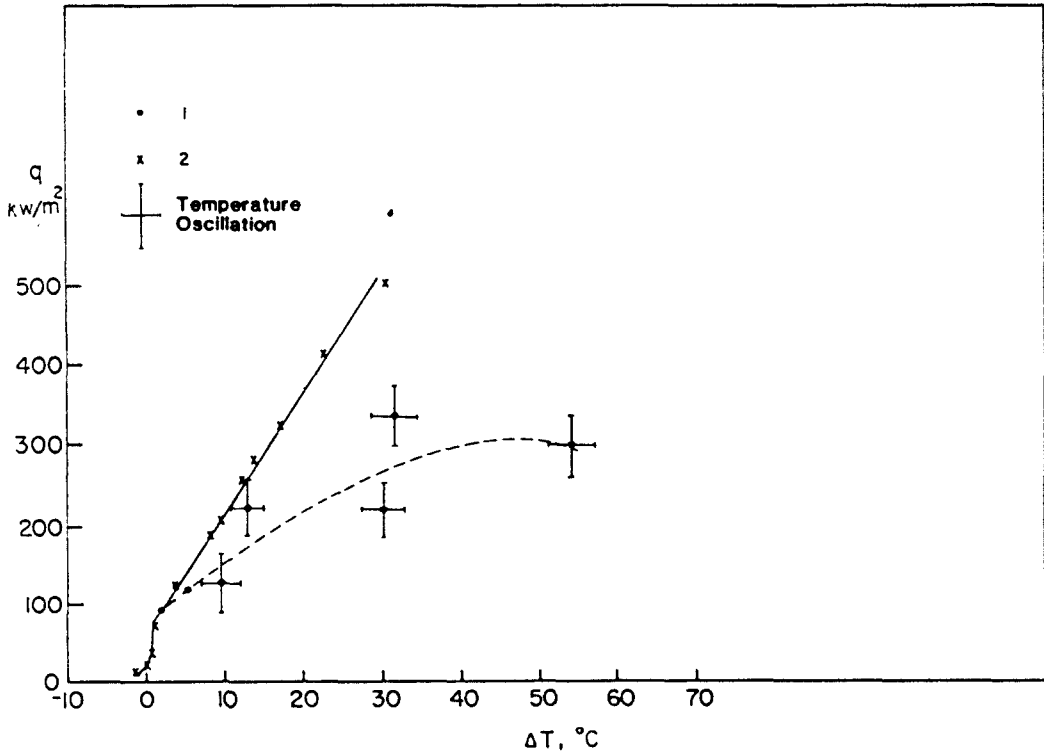


Figure 8. Effect of inlet quality on concentric narrow gap boiling.

Symbol	G , $\text{kg/m}^2\text{s}$	Inlet quality subcooling $^{\circ}\text{C}$	Pressure 10^5 n/m	Gap, mm
1	330	0.14	1.3	0.317
2	330	8 $^{\circ}\text{C}$	1.3	0.317

Unlike the case of flow boiling in a tube, where higher pressures result in lower ϕ^2 , here the opposite is observed. Another peculiar result is that with smaller gaps ϕ^2 is considerably lower. Additional theoretical and experimental studies are required to verify and explain these effects.

When comparing the two-phase pressure drop multiplier obtained here (ϕ^2) with the homogeneous multiplier given in Collier (1981):

$$\phi_{\text{hom}}^2 = 1 + (\rho_l/\rho_v - 1)x \quad (2)$$

it is found that $\phi^2 < \phi_{\text{hom}}^2$.

4. SUMMARY

Four different boiling regimes were identified in forced convective boiling in a concentric annular gap:

- Isolated bubble
- Coalesced bubbles with a thin liquid film remaining on the tube surface
- Coalesced bubbles with small unstable dry patches
- Liquid deficient regime

The last two regimes result in surface temperature fluctuations that increase in amplitude and frequency as the wall superheat increases.

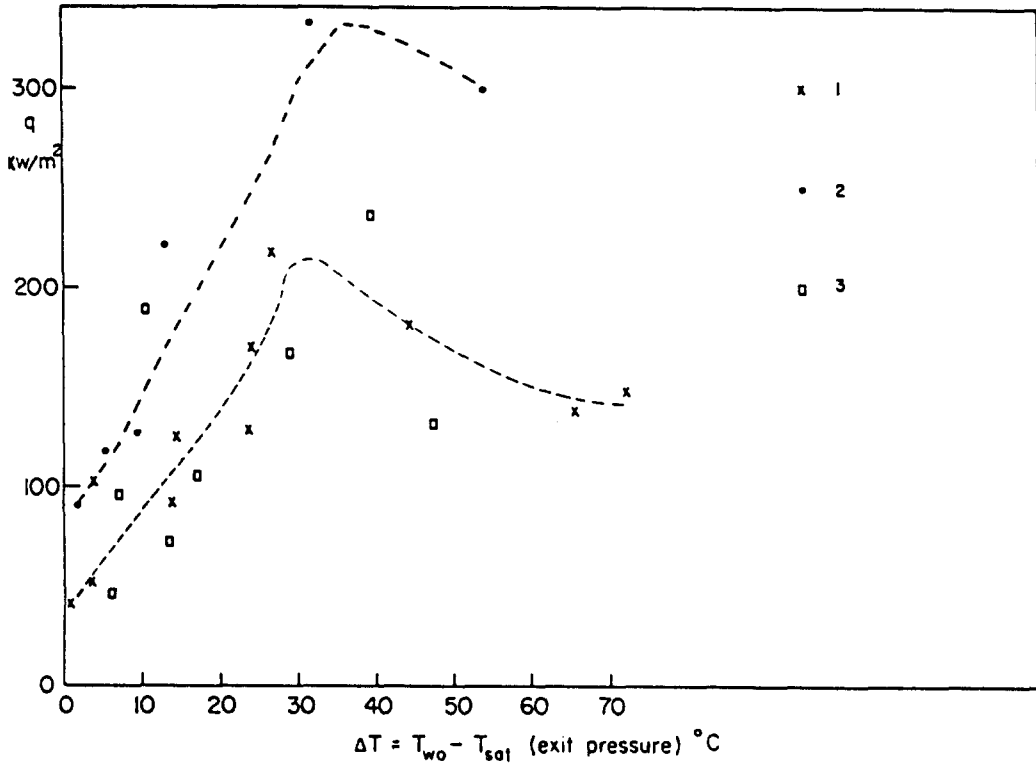


Figure 9. Effect of gap size on concentric narrow gap boiling. All temperatures oscillate above $\Delta T \sim 10^\circ\text{C}$.

Symbol	$G, \text{kg/m}^2\text{s}$	Inlet Quality	Pressure 10^5 n/m^2	Gap, mm
1	330	0.15	1.3	0.191
2	330	0.14	1.3	0.317
3	330	0.14	3	0.191

Isolated bubbles appear with the larger gap (0.317 mm) at subcooled or low quality inlet conditions. With the smaller gap (0.191 mm) this regime occurs only at the incipience of boiling.

The transition to the coalesced-bubble regime depends on mass velocity, gap size, wall superheat and inlet quality. Smaller mass velocity and gap size, and larger wall superheat and inlet quality favor this transition. The transition gap size is much smaller in convective boiling compared with pool boiling (3 mm at 1 atm). In convective flow this transition depends largely on wall superheat, while in pool boiling (Ishibashi & Nishikawa 1969) no such effect is reported. The coalesced bubble regime has several new features:

(a) The heat flux in subcooled boiling is an inverse function of pressure at constant temperature difference, as found also in pool boiling.

(b) Coalesced-bubble boiling leads to a smaller heat transfer coefficient compared to normal convective boiling. As a result the boiling curve is much flatter in this regime. This result holds both with subcooled and with saturated inlet conditions.

(c) In subcooled boiling no "lubrication effects" of bubbles on the wall shear stress are observed. Hence the two-phase pressure drop multiplier always increases with heat flux.

(d) In subcooled boiling a smaller gap results in a higher ϕ^2 . However, in saturated boiling with $x_{in} = 0.14$, the opposite effect is observed. More data are required to verify these preliminary results.

(e) Increasing pressure seems to increase ϕ^2 for the same (positive) average quality in the gap. This is opposite to normal saturation boiling pressure drop behavior.

The liquid deficient regime is observed with higher inlet quality, smaller gap and larger wall

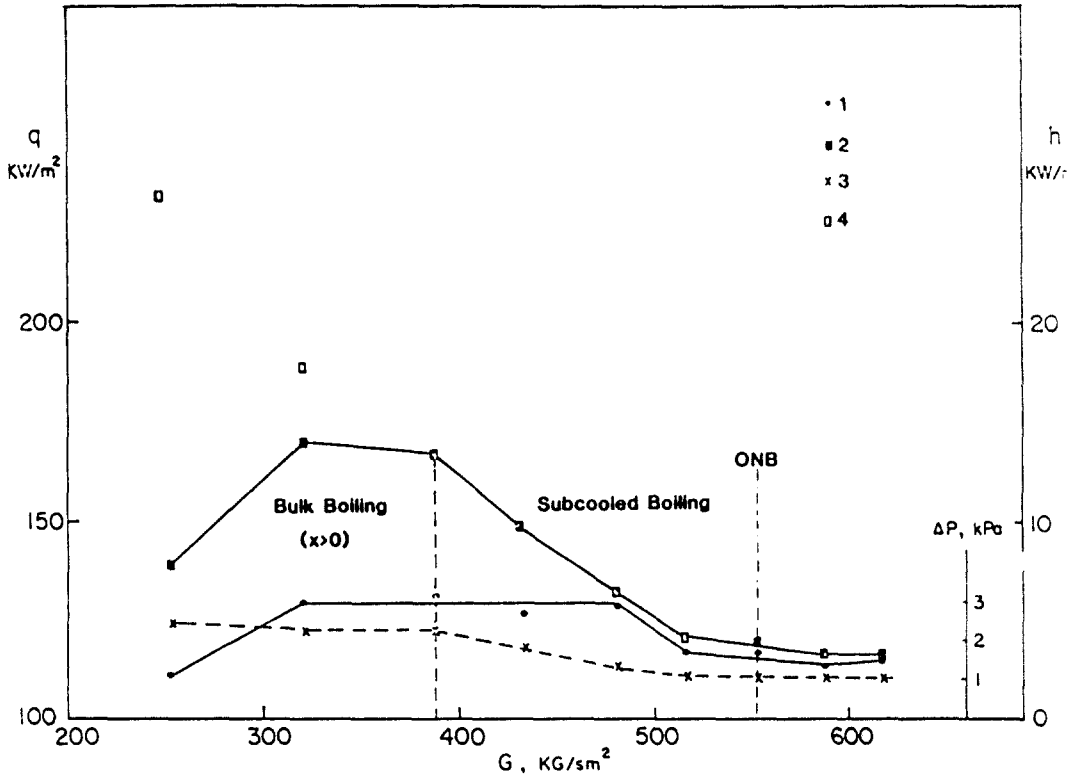


Figure 10. Combined effect of mass velocity and quality on the concentric narrow-gap boiling heat transfer. $P = 0.3$ MPa, $T_p = 160$, 0.317 mm gap: 1, heat flux; 2, heat transfer coefficient; 3, pressure drop; 4, heat transfer coefficient calculated by Chen correlation.

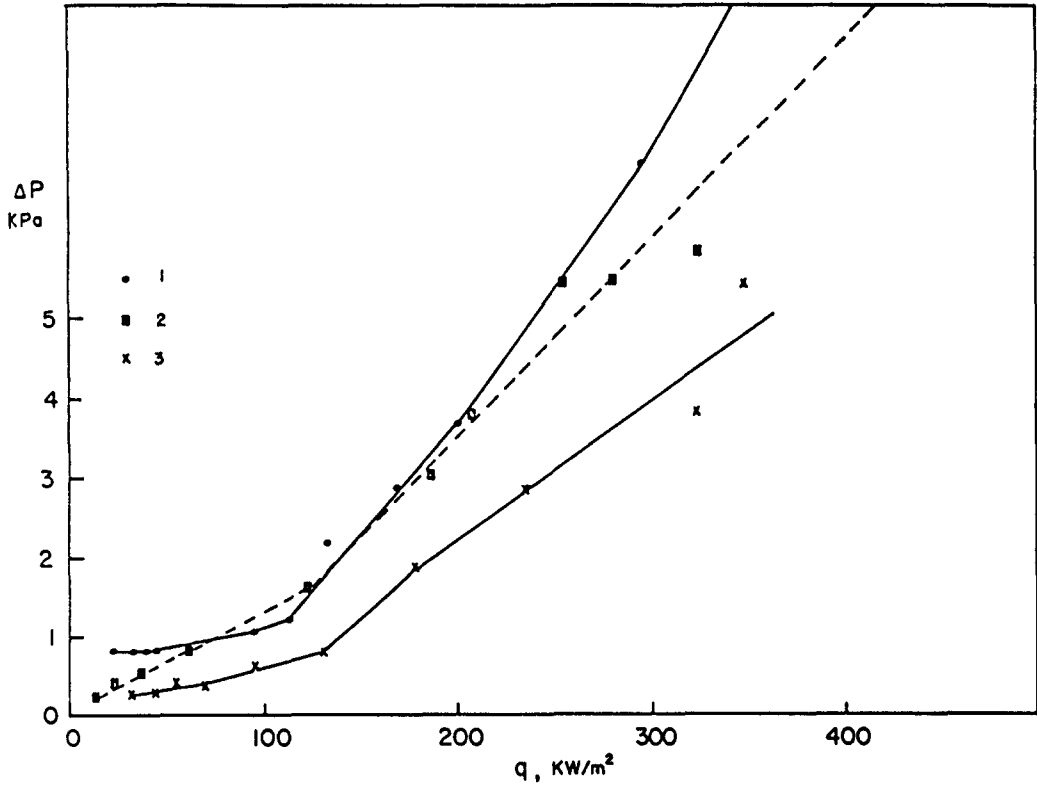


Figure 11. Effect of mass velocity on pressure drop in concentric narrow-gap subcooled boiling.

Symbol	$G, \text{kg/m}^2\text{s}$	Inlet subcooling $^{\circ}\text{C}$	Pressure 10^4 n/m^2	Gap, mm
1	570	12	3	0.317
2	330	8	1.3	0.317
3	330	14	3	0.317

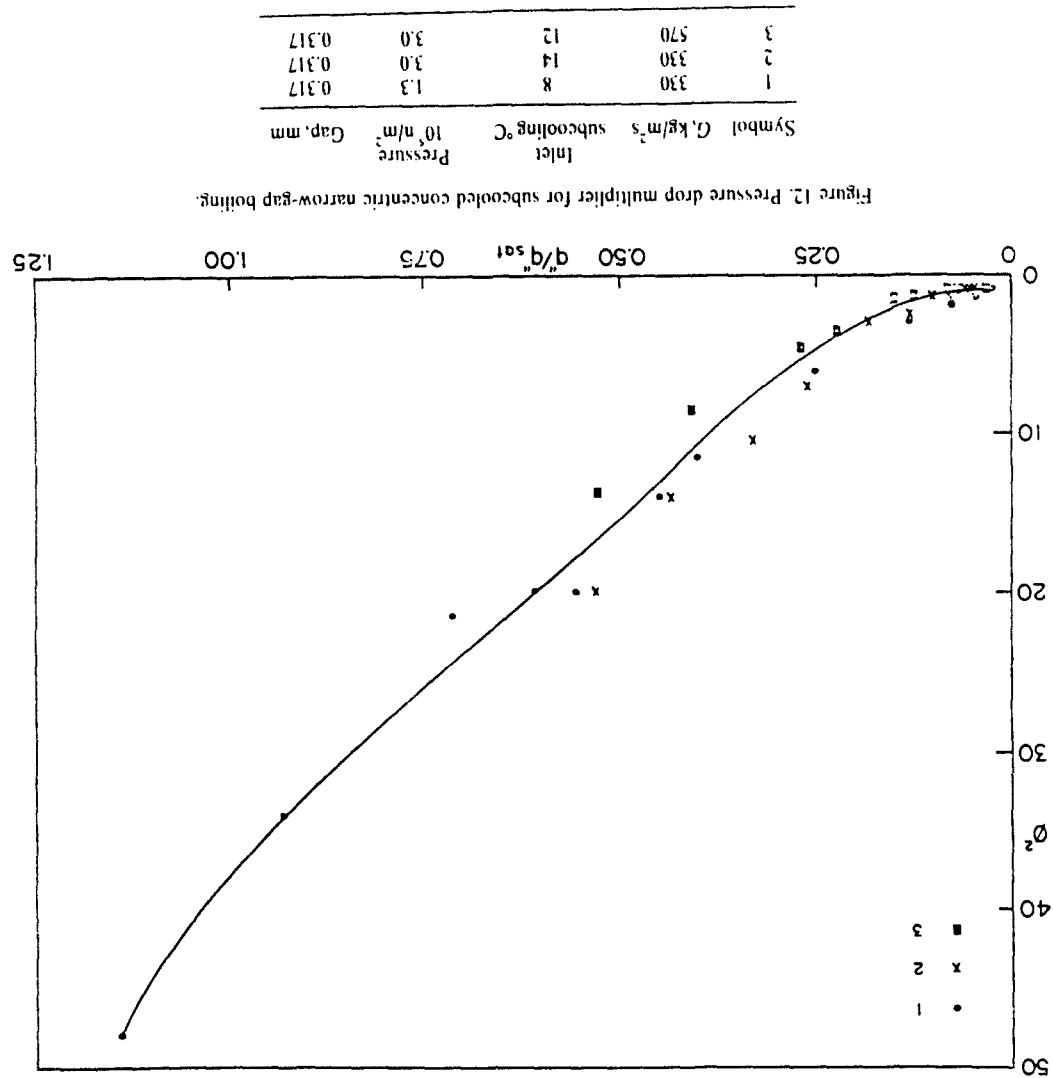


Figure 12. Pressure drop multiplier for subcooled concentric narrow-gap boiling.

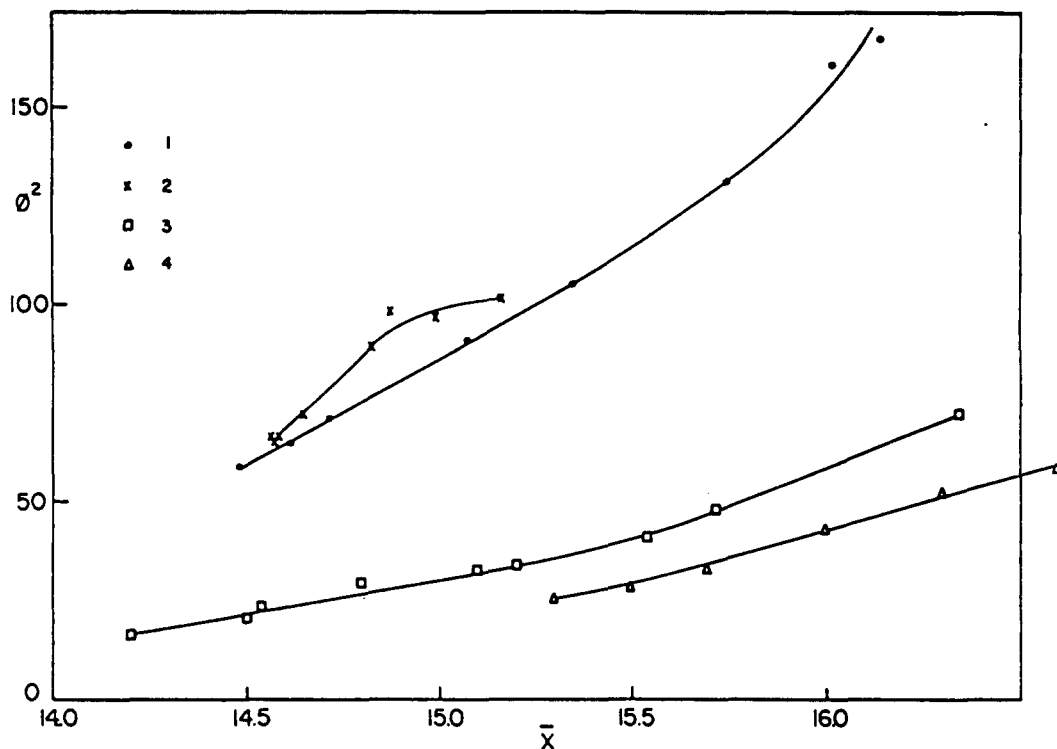


Figure 13. Pressure drop multiplier for saturated concentric narrow-gap boiling.

Symbol	$G, \text{kg/m}^2\text{s}$	Inlet quality	Pressure 10^4 n/m^2	Gap, mm
1	330	0.145	1.3	0.191
2	570	0.141	3	0.191
3	330	0.138	3	0.317
4	330	0.15	1.3	0.317

superheat. The heat flux usually decreases with large wall superheat, leading to a maximum in the boiling curve.

The data reported here covers only a limited range and are presented to illustrate the characteristics of the boiling regimes associated with this special boiling mode. However, the data so far suggest that the *unconfined forced convective correlations* recommended by Collier (1981) for either heat transfer or pressure drop are not applicable for narrow gap boiling. More data are required to establish working correlations for forced convection boiling in a narrow concentric annulus.

Acknowledgments—This equipment was originally constructed under a contract with Electric Power Research Institute (EPRI) with Drs. C. L. Williams and G. Hetsroni as project managers. Dr. P. Kalra was the project manager for the present work. Support for Mr. L. Chen was provided by the Peoples Republic of China. The original design was drawn up by Dr. Y. Kozawa of the Tokyo Institute of Technology under a grant from the Japanese government while a Visiting Scholar at Northwestern University. For all these contributions we offer our thanks.

REFERENCES

BANKOFF, S. G. TANKIN, R. S., YUEN, M. C., JOHNSTON, B. S., KOZAWA, Y. & SHARON A. 1982 Boiling heat transfer in a narrow eccentric annulus. EPRI report EPRI NP-2610.
 BAUM, A. J. & CURLEE, N. J. 1980, An experimental and analytical investigation of dryout and chemical concentration in confined geometries. ASME Century 2 Nuclear Engineering Conference, San Francisco.

- COLLIER, J. G. 1981, *Convective Boiling and Condensation*. McGraw-Hill, New York, 2nd Edition.
- ISHIBASHI, E. & NISHIKAWA, K. 1969, Saturated boiling heat transfer in narrow spaces. *Int. J. Heat Mass Transfer* 12, 863–865.